PRELIMINARY NUMERICAL MODELING OF BRINE FORMATION ON MARS DURING IMPACT-DRIVEN HYDROTHERMAL CIRCULATION: THE CHESAPEAKE BAY ANALOG.

Pavithra Sekhar[1] and Robert. P. Lowell[2], Virginia Polytechnic Institute and State University (Department of Geosciences, 4044 Derring Hall (0420), Blacksburg, VA 24061; [1]pav06@vt.edu, [2]rlowell@vt.edu).

Introduction: Even though there is little water vapor present in the Martian atmosphere [1] and liquid water is unstable on the Martian surface [2], there is abundant evidence that liquid water was present at the surface earlier in the planet's history. There is also evidence of recent groundwater seepage [3], and it is widely accepted that water is stored beneath the Martian surface either as solid-state ice [4], as clathrates [5,6] or in liquid form [7]. If liquid water exists below the Martian surface, it likely occurs as a thermodynamically stable saline brine [8]. The formation of brines on Mars has been related to evaporative processes from the Martian surface [8]. But brines can also be formed during boiling and phase separation of a saline fluid as a result of high-temperature magma-driven hydrothermal circulation [9], during convection and near surface freezing of saline groundwater [10], and during impact-driven hydrothermal flow. To explore the possibility of brine formation and storage on Mars, we construct a 2-D numerical model of two-phase flow in a $NaCl$-H_2O hydrothermal system driven by an impact event. This is the first attempt to model two-phase flow and brine formation in an impact-driven hydrothermal system using a $NaCl$-H_2O fluid.

Modeling: In order to constrain the numerical model for brine formation during an impact-driven Martian hydrothermal system, we model two-phase $NaCl$-H_2O hydrothermal circulation associated with the Chesapeake Bay impact event [11] using the numerical simulator FISHES [12,13]. FISHES uses the finite volume method [14] to solve the equations that describe conservation of mass, momentum, and energy in a $NaCl$-H_2O system [15] and the equation that describes conservation of salt [16]. This code has been previously used to model phase separation in hydrothermal systems at mid-ocean ridges [17,18]. The model geometry shown in Figure 1 depicts a 6 km deep by 40 km wide system similar to that of [11] consisting of square cells of 500 m size in the x-axis and y-axis. This model geometry represents one half of the impact crater along with its rim. We assume the whole crater to be 40 km wide and 2 km deep with a rim of 5 km. The surface is assumed to be overlain by a 1 km thick layer of seawater, so the surface pressure and temperature are held constant at 10 MPa and 10°C, respectively. The constant pressure upper boundary permits free fluid exchange. Consequently we apply upstream weighting boundary condition on the temperature and salinity of fluid entering or leaving the upper boundary. The bottom boundary is impermeable and maintained at constant temperature. The left and right hand boundaries are insulated and impermeable.
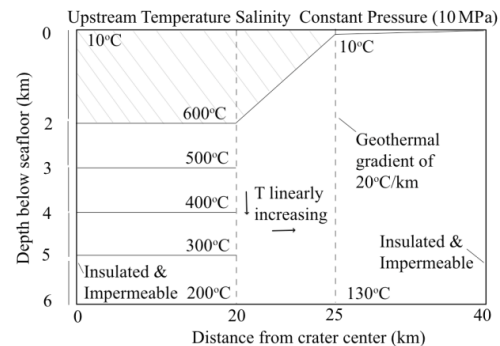

Figure 1: Model setup in FISHES

The system is divided into three sections for modeling purpose. The left section (zone 1) contains the base of the crater at a depth of 2 km and width of 20 km with a temperature gradient of 295°C/km. Beneath the crater; we assume that the gradient decreases by 100°C/km. The middle section (zone 2) of the system contains the 5 km wide rim of the crater. In this zone, there is a linear increase in temperature horizontally and vertically. The right section (zone 3) contains the colder part of the system, where the geothermal gradient of the system is 20°C/km. We assume the system has a uniform permeability of 10^{-16} m^2 (Figure 1).

Results: To investigate phase separation and the formation of brine in this system, we simulated hydrothermal circulation for 500 years.
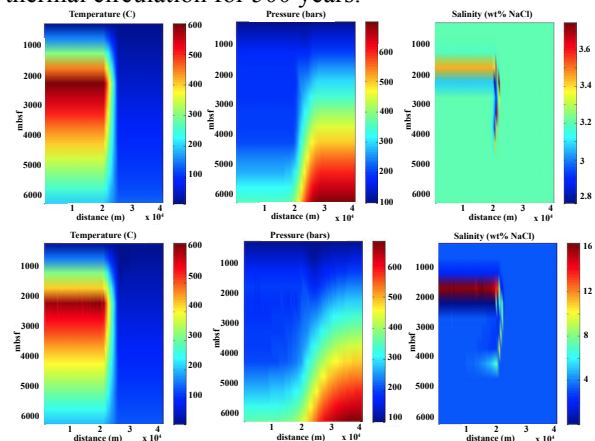

Figure 2: Temperature, pressure and salinity at 1 yr (top) and 500 yr (bottom) of simulation time for the geometry in Figure 1.

Figure 2 shows the temperature, pressure and salinity distribution after the initial step (1 year) and final step (500 years) of the model. The temperature distribution has changed relatively little during 500 years of the simulation. In addition, the pressure distribution shows a low pressure in zone 1 that results from the high temperature and formation of low-density vapor beneath the crater. The salinity plot (top right) shows the development of a two-phase system where brine and vapor is formed at the crater boundary and beneath the crater. As the model evolves (bottom image), the brine layer formed near the bottom of the crater has increased in salinity and low-density vapor occurs both beneath and above the brine. In addition brine formed near the edge of the crater tends to sink and grow laterally at depth.

The isotherm distribution and velocity vectors in zones 1 and 2 were analyzed. The velocity vectors show convection driven by the large lateral temperature gradient associated with the crater rim. The velocity plot also shows brine sinking and vapor rising beneath the crater. The rising vapor transports heat upward beneath the crater while thermal conduction and brine formation tend to transport heat downward. These interactions tend to maintain the thermal regime in quasi-steady state and modulate the salinity within the brine layer.

Discussion: These preliminary model simulations show clear evidence of phase separation and two-phase flow. The results show that a several hundred meter thick brine layer forms beneath the crater whose salinity increases with time. Increasing the permeability to 10^{-15} m^2 (Figure 3) results in a more vigorous convection system so that the convection in zone 2 move further beneath the crater. A plume of vapor rises toward the surface near the right
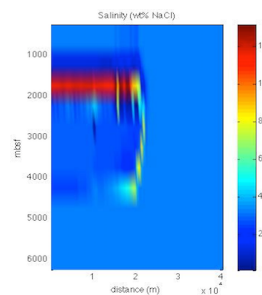

Figure 3: High permeability model at 100 years

boundary of the crater. The vapor above the brine layer is more pronounced and the sinking of brine in the region of vigorous convection near the edge of the crater is more rapid. The results in Figure 3 at 100 years, compared to the results in Figure 2 at 500 years indicates that increasing the permeability strongly affects brine formation and the dynamics of the convection system.

Conclusion: These preliminary simulations have run for a relatively short time. They do not show the expected cooling with time, in part because of the low permeability assumed and also because of the interactions between rising vapor and sinking brine beneath the crater. Previous modeling of two-phase hydrothermal circulation in Chesapeake Bay Crater used pure water [11]; and it took 100000 years for the system to reach near hydrostatic pressures. Therefore, our models represent an early stage of evolution. The models do show the formation of a significant brine layer, suggesting that the brines observed beneath the Chesapeake Bay Crater could have been produced by two-phase flow of seawater during impact-driven hydrothermal circulation. Similar processes of brine formation could have also occurred on Mars. Further modeling that covers a broader range of parameter space and runs for longer times are needed to explore the evolution and ultimate fate of brines formed during impact-driven hydrothermal circulation. Higher resolution modeling would also provide a clearer picture of brine evolution in the system.

References:
[1] Baker (2001) *Nature, 412*, 228-236. [2] Jakosky and Phillips (2001) *Nature, 412*, 237-244. [3] Malin and Edgett (2000) *Science, 288*, 2330-2335. [4] Plaut et al (2007) *Science, 316.* [5] Max and Clifford (2000) *JGR, 105*, 4165-4171. [6] Max and Clifford (2001) *GRL, 28*, 1787-1790. [7] Haberle et al (2001) *JGR, 106,* 23,317-23,326. [8] Knauth and Burt (2002) *Icarus 158,* 267-271. [9] Bischoff and Pitzer (1989), *American Journal of Science, 289,* 217-248. [10] Travis et al (2013) *JGR 118, 877-890* [11] Sanford (2005) *Geofluids 5,* 185–201. [12] Lewis and Lowell (2009a) *JGR, 114*, B05202. [13] Lewis and Lowell (2009b) *JGR, 114*, B08204. [14] Patankar (1980) 197, *Taylor and Francis, London.* [15] Faust and Mercer (1979) *Water Resour. Res., 15*, 23–30. [16] Bai et al. (2003) *GRL, 30(3)*, 1108. [17] Han et al (2013) *JGR, 118,* 2635–2647. [18] Singh et al (2013) *Geochem, Geophy, Geosys. 14,* 4021-4034.